Objective frontal analysis applied to the extreme/non-extreme precipitation events

Marek Kašpar

Institute of Atmospheric Physics AS CR, Bocni 2, 14131 Prague 4, Czech Republic;

e-mail: kaspar@ufa.cas.cz

Fig. 1.

OBJECTIVE ANALYSIS OF FRONTS AND VERTICAL VELOCITY IN THE ATMOSPHERE (1000 gpm ABOVE TOPOGRAPHY)

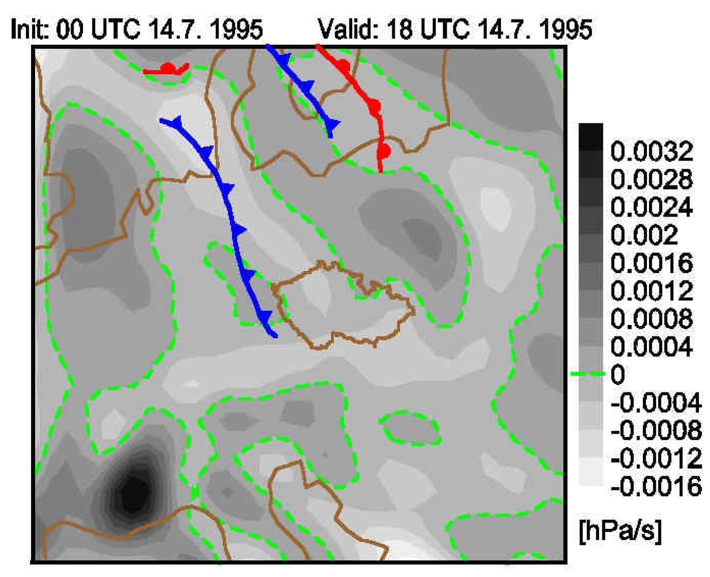

Fig. 2.

OBJECTIVE ANALYSIS OF FRONTS AND VERTICAL VELOCITY IN THE ATMOSPHERE (500 hPa LEVEL)

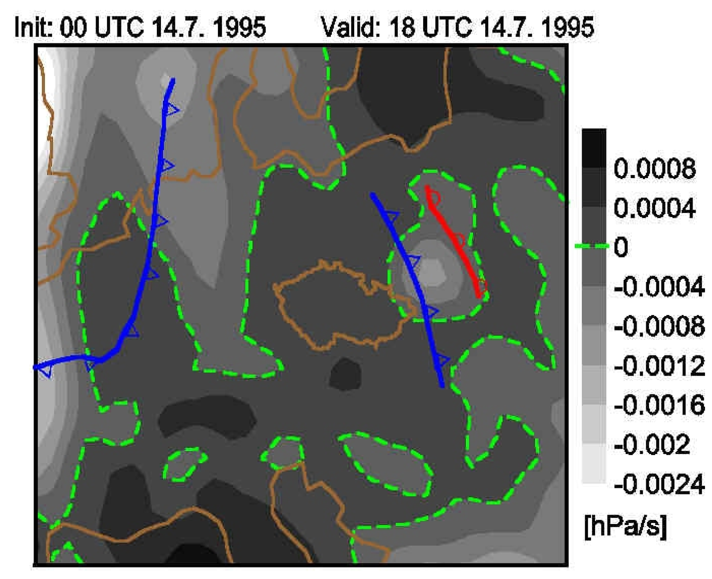

Fig. 3.

FRONTOGENETICAL FUNCTION (FR) ALONG OA FRONTS AND OBJECTIVE ANALYSIS OF VERTICAL GRADIENT OF EQUIVALENT POTENTIAL TEMPERATURE (1000 gpm ABOVE TOPOGRAPHY)

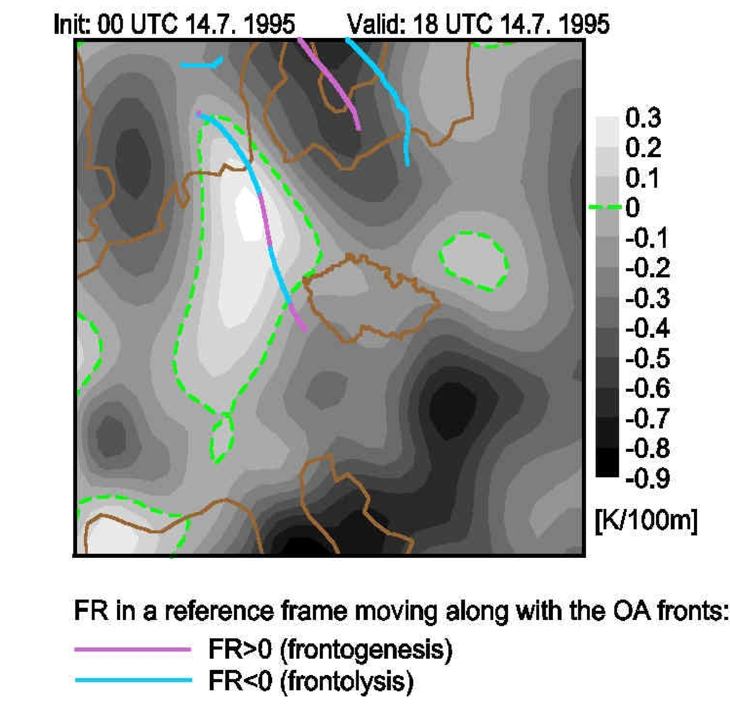

Fig. 4.

FRONTOGENETICAL FUNCTION (FR) ALONG OA FRONTS AND OBJECTIVE ANALYSIS OF VERTICAL GRADIENT OF EQUIVALENT POTENTIAL TEMPERATURE (500 hPa LEVEL)

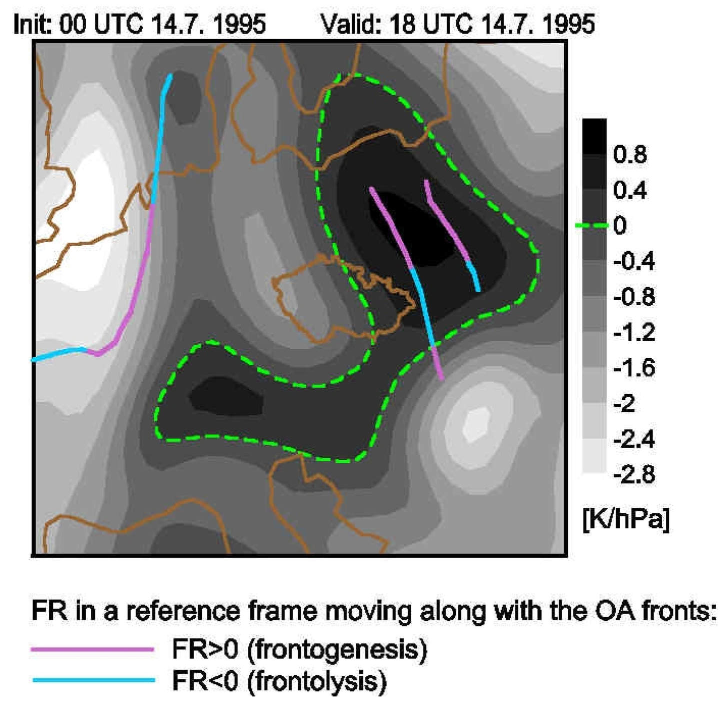

Fig. 5.

OBJECTIVE ANALYSIS OF THE SPEED OF FRONTAL MOVEMENT AND EQUIVALENT POTENTIAL TEMPERATURE

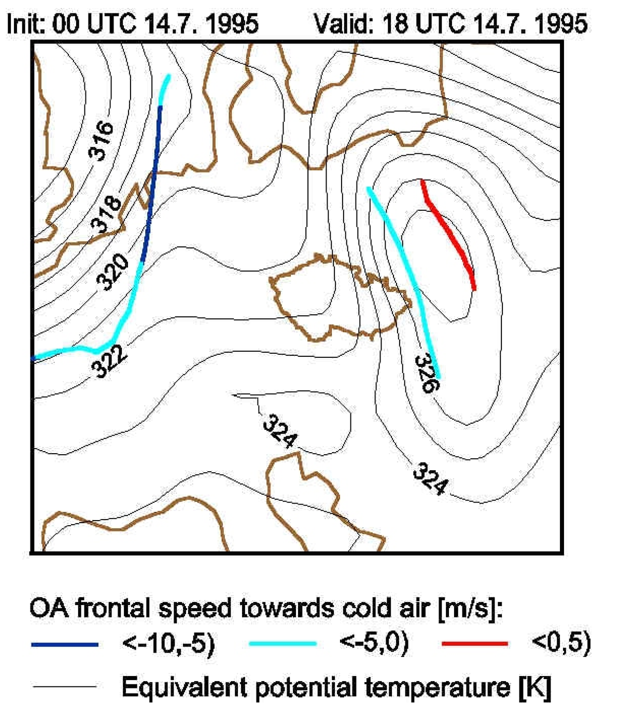

Fig. 6.

OBJECTIVE ANALYSIS OF FRONTS (1000 gpm ABOVE TOPOGRAPHY) AND GEOPOTENTIAL HEIGHT OF 925 hPa LEVEL

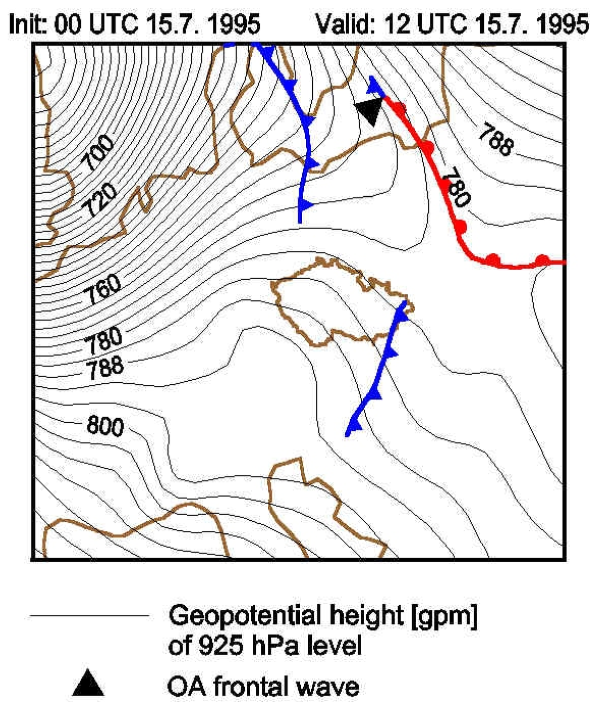

Fig. 7.

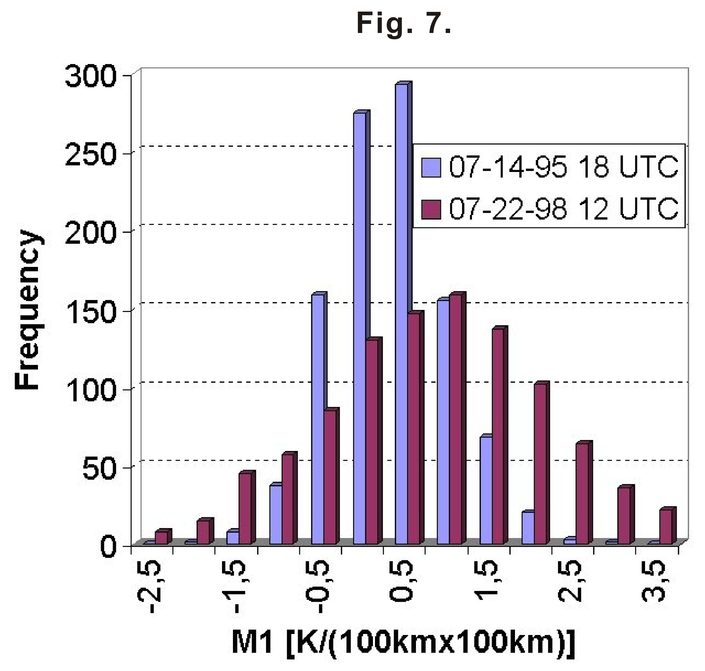

Fig. 8.

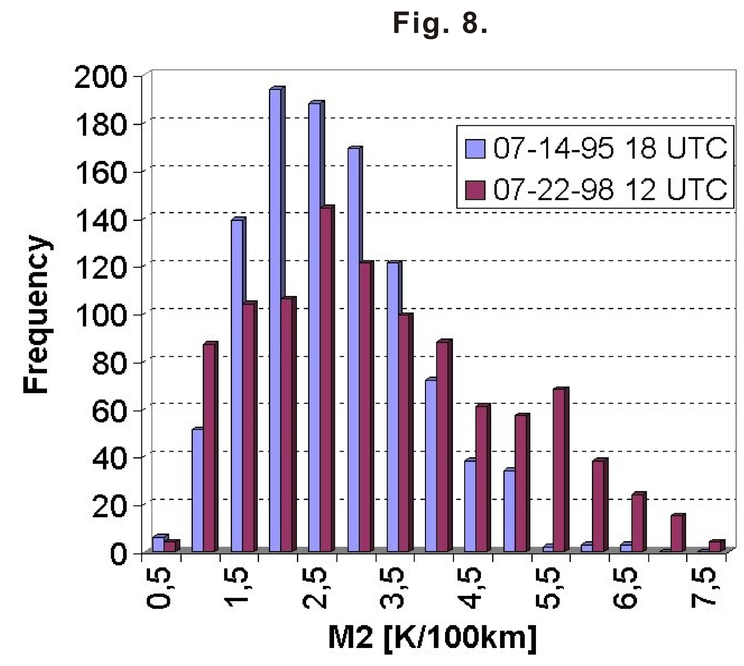

Fig. 9.

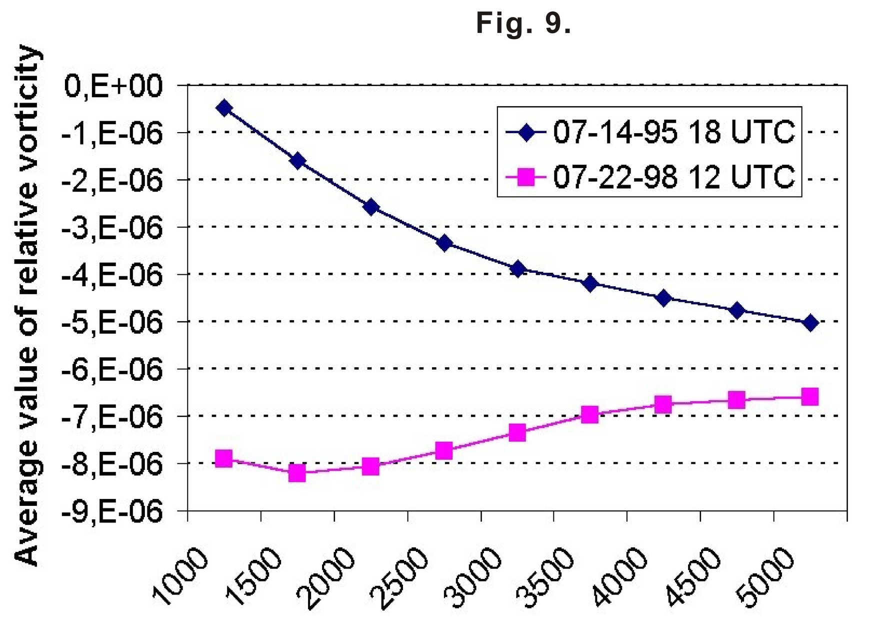

1. INTRODUCTION

A simple method of the objective frontal analysis (**OFA**) based on a thermal definition of atmospheric fronts is proposed for the area of Central Europe. The OFA includes both mathematical and graphical techniques that enable a computer to draw fronts entirely automatically in atmospheric cross-sections by means of one locating equation and four masking criteria. The OFA also enables to analyse the frontal wave position and the type, activity, and future development of fronts. The OFA is applied to two synoptically analogous cold-frontal situations, which occurred over the Czech Republic (**CR**) in summer season and were characterised by quite different precipitation amounts. The prognostic outputs of the NWP model *Europa Modell/Deutschland Modell* (**EM/DM**) are used in computations. The subjective frontal analyses helped to optimize the masking threshold constants. For the examined cases, the comparison of the analysed situations with the aid of the OFA is presented. The stress is laid on the OFA products that support (or do not support) the forecast of enhanced precipitation amounts. The distribution parameters of the threshold constants are also compared.

2. FUNDAMENTAL FEATURES OF THE OFA

The OFA was developed on the basis of the method described in [6] and [7]. In the following text, the resultant products of the OFA will be indicated by the abbreviation **OA**.

A. Spatial location of OA fronts

The presented OFA employs selected diagnostic quantities together with the graphical techniques to plot atmospheric fronts without human intervention. The OFA determines the frontal position by means of one locating equation and four masking criteria (variables).

A1. Front locating variable (L)

An OA front is defined as a line, adjacent to a baroclinic zone, across which the magnitude of the thermal gradient is changing most abruptly:

$(L)\quad L \quad | \quad |_{\hat{s}} / \hat{s} \quad 0,\ \hat{s} \quad | \quad |/| \quad | \quad \|,$

where is a thermal variable, $\hat{s}$ is a 'unit axis', and is the operator of the horizontal gradient. This definition is analogous to the thermodynamic definition of objectively localised fronts originally published by *Renard and Clarke* [11].

A2. Masking variables (M1-M4)

(*M1*) The rate of change of the thermal gradient across the OA front must be greater than a pre-defined critical value K_1.

(*M2*) The thermal gradient in the baroclinic zone adjacent to the OA front must be greater than a pre-defined critical value K_2.

(*M3*) Humidity index *HIX*, which specifies the degree of water vapour saturation of 850-500 hPa layer [8], must be greater than a pre-defined critical value K_3.

(*M4*) Relative vorticity must be greater than a pre-defined critical value K_4.

The various settings of the masking threshold constants K_1 to K_4 enable to distinguish weaker fronts (less active) from stronger fronts.

B. Products of the OFA

(I) **Warm and cold OA fronts**: The segments of OA fronts, where the local thermal advection *A* is negative and positive, are analysed as cold and warm OA fronts, respectively.

(II) **OA frontal waves**: The OA frontal wave is localised along the OA front, where *A* equals zero and the angle between an along front vector with warm air to the right and a vector of the horizontal gradient of *A* is less then 90.

(III) **OA frontal speed of movement**: The OA frontal speed is given by the magnitude of the horizontal wind component in a direction perpendicular to the OA front and into colder air.

(IV) **Frontogenesis and frontolysis of OA fronts**: The segments of the OA front, where the frontogenetical function in a reference frame moving along with the OA front is positive and negative, undergo frontogenesis and frontolysis, respectively.

(V) **OA anafronts and katafronts**: The segments of OA fronts, where the quasi-geostrophically forced part of the vertical motion in z-coordinate system is positive and negative, are analysed as OA anafronts and OA katafronts, respectively.

C. Other thermodynamic quantities combined with the OFA

Apart from the thermal and humidity characteristics of the airmass within the frontal zone, the stability conditions also affect the activity and further development of atmospheric fronts.

(I) **Potential instability**: The layer of air is potentially unstable, when the vertical (pressure) gradient of the equivalent potential temperature $_e$ is negative (positive).

(II) **Conditional instability**: When the layer has potential energy for convection, it is conditionally unstable (unstable upon the saturation conditions). In this case, the convective available potential energy *CAPE* is defined and its value is greater than zero.

(III) **Conditional symmetric instability**: The necessary condition for the instability is that the analogue (for moist air) of Ertel's potential vorticity is negative [2]. When the layer has potential energy for slantwise convection, it is conditionally symmetric unstable. In this case, the slantwise convective available potential energy *SCAPE* is defined and its value is greater than zero.

3. COMPUTATIONS

The prognostic outputs of the workstation version of the German NWP model *Europa Modell* (**EM**, included in EM/DM package [4]) were used in OFA computations. The EM model domain covers the greater part of Europe and consists of 41×37 gridpoints on a 0.5° latitude-longitude grid and 20 hybrid vertical levels. Initial and boundary conditions were obtained from the objective analysis of aerological measurements from European stations [13]. The model was applied with the Eulerian integration scheme using a time step of 300 s, adiabatic initialization by normal modes, and physical parameterizations of vertical diffusion, convection, grid-scale precipitation, and radiation.

Before computations a horizontal digital filter was applied to the model outputs. The filter removes all the waves with wavelengths smaller than four times the gridlength ([4], [12]). In the calculations with derivative operators, the simple first order finite differencing was used. For simplicity, the trapezoidal rule was used in the calculations of integrals. The gridded dataset for $_e$ was considered as an input thermal field . Surface OA fronts were analysed at the level, whose geopotential height above topography is everywhere 1000 gpm. Upper OA fronts were analysed at 500 hPa level.

4. APPLICATIONS OF THE OFA TO SYNOPTICALLY ANALOGOUS COLD-FRONTAL SITUATIONS

The analysed cases occurred in summer season and were characterised by the passage of a cold front across the CR. The fronts associated with the driving cyclone centred over British Isles. Ahead of the fronts, there prevailed a south to south-west flow of very warm and moist tropical air. The situations were accompanied with extreme (22-23 July 1998) and non-extreme (14-15 July 1995) precipitation amounts.

A. Situation 1: 22 - 23 July 1998 (Flood episode)

The examined cold front moved slowly eastwards across the CR during 22 July 1998. The front lay within the shallow pressure trough. In the afternoon the front began to wave and its advance still slowed down. The first thunderstorms appeared near the mesoscale frontal wave at 16 UTC. The heavy thunderstorms lasted about 10 hours and caused flash flood in the north-east of the CR. The highest precipitation sums were detected in the strip 50 km long and 20 km wide [5]. In the morning on 23 July the frontal advance again sped up and the front left the CR. The daily precipitation maximum enhanced by mesoscale convective organization reached the value of 204 mm [9]. Before forming thunderstorms the methods of the classical synoptic meteorology did not indicate the possibility of such high precipitation amounts.

The EM model was integrated for the initial analysis from 00 UTC 22 July. The OFA was applied to the prognostic fields from 12 h forecast and 24 h forecast. The results that supported the forecast of enhanced precipitation amounts can be summarized as follows (these results with the relevant graphical products of the OFA were already presented in [10].):

(I) Anafrontal character of the cold front combined with sufficient humidity ahead of the front.

(II) Potentially unstable tropical air and the high energy of instability in the vicinity of the cold front (*CAPE*~1700 J/kg).

(III) Low speed of movement of the cold front (10 ms^{-1}).

(IV) Appearance and development of a frontal wave and the resultant almost stationary position of the cold front (5 ms^{-1}).

B. Situation 2: 14 - 15 July 1995

The examined cold front began to affect the territory of the CR from the west in the evening on 14 July 1995. The first local frontal showers and thunderstorms appeared at 18 UTC. During night the front advanced rapidly towards the east to south-east. In the early morning on 15 July the frontal surface was already positioned in the eastern part of the CR, where its advance temporarily sped down and the front commenced to decay. Precipitation sums reported by the most meteorological stations from 06 UTC 14 July till 06 UTC 15 July did not exceed 10 mm. Some mountain stations measured the maximum precipitation sums up to 40 mm.

The EM model was integrated for two initial analyses from 00 UTC 14 July and 00 UTC 15 July. The OFA was applied to the prognostic fields from 18 h forecast (valid at 18 UTC 14 July) and 24 h forecast (valid at 00 UTC 15 July) for the first initial analysis and to the fields from 12 h forecast (valid at 12 UTC 15 July) for the latter. Several examples of the graphical products of the OFA combined with some meteorological quantities are showed in Figs. 1 to 6. From the comparison with the flood episode with the aid of the OFA, many identical features were obvious. Nevertheless, a few differences, which did not support the forecast of enhanced precipitation amounts, became evident and can be summarised as follows:

(I) Less compact and vertically extensive layer of tropical air ahead of the cold front (Fig. 5).

(II) Katafrontal character of the southern part of the cold front, which affected the Czech region (Figs. 1 and 2).

(III) Shallow layer of slightly potentially unstable air (Figs. 3 and 4) and the lower energy of instability in the vicinity of the cold front (*CAPE*=(600,1100) J/kg).

(IV) No appearance of any frontal wave at the cold front (Figs. 1, 2, and 6) and the successive decay of the front, especially its northern part (Figs. 3, 4, and 6).

5. MASKING THRESHOLD CONSTANTS

The masking threshold constants were subjectively set to reach the best accordance of the OFA graphical products with the Czech [3] and German [1] subjective frontal analyses. Table 1 shows the values of the threshold constants that were used in the OFA. The masking criteria are maximally severe not to affect the resultant OA fronts that are also presented in the subjective frontal analyses.

The comparison of the 'optimal' (maximal possible) threshold constants between the examined situations (table 1) exposes that the frontal surface was thermally stronger in the case of the flood episode. In addition, the degree of water vapour saturation of 850-500 hPa layer (expressed by *M3*) within the frontal zone was slightly lower for the flood episode. The masking criterion using *M1* has the maximal effect on the graphical products of the OFA and the criterion using *M2* has the minimal effect.

Table 1

Date of forecast	*Atmospheric level*	*Threshold constant* $K1$ [K/(100km)^2]	$K2$ [K/100km]	$K3$ [ ]	$K4$ [s^{-1}]
07-14-1995 18 UTC	*1000 gpm*	0.28	2.18	0.77	-1.25
	500 hPa	0.29	0.96	0.78	-1.27
07-15-1995 12 UTC	*1000 gpm*	0.45	1.65	0.78	-1.16
07-22-1998 12 UTC	*1000 gpm*	1.22	3.03	0.75	-1.00
	500 hPa	0.55	1.84	0.77	-2.24

Since the highest distinction between the situations are for the threshold constants K_1 and K_2, the values of the thermal masking variables *M1* and *M2* in model domain were investigated in detail. The statistics of *M1* and *M2* for 1000 gpm level at forecast terms, which closely preceded the passage of the cold front across the CR, are in table 2. The relevant histograms are depicted in Figs. 7 and 8.

Table 2

Statistic	*Masking variable and date of forecast (1000 gpm level)* $M1$ [K/(100km)^2] *07-14-1995 18 UTC*	$M1$ *07-22-1998 12 UTC*	$M2$ [K/100km] *07-14-1995 18 UTC*	$M2$ *07-22-1998 12 UTC*
Number of data	1020	1020	1020	1020
Average	0.063	0.051	2.427	3.016
Median	0.052	0.050	2.322	2.729
Variance	0.469	1.085	1.056	2.491
Minimum	-2.32	-2.66	0.42	0.42
Maximum	2.76	3.06	6.50	7.29
Lower quartile	-0.407	-0.619	1.642	1.748
Upper quartile	0.466	0.750	3.056	4.106
Skewness	0.213	0.025	0.598	0.475
Kurtosis	0.394	-0.190	0.201	-0.649
Equality of averages (significance level 5 %)	YES		NO	
Equality of variances (significance level 5 %)	NO		NO	

The variance of the values of *M1* is greater for the flood episode (table 2 and Fig. 7). The difference of the variances between the situations is statistically significant. The greater variance for the flood episode can explain more severe masking criterion using *M1* (higher value of K_1) because the impact of the criterion on the resultant graphical products of the OFA is thus less. The distribution of the values of *M1* is almost symmetric in both cases.

The average and variance of *M2* are greater for the flood episode (table 2 and Fig. 8). The differences of the averages and variances between the situations are statistically significant. The greater average and variance for the flood episode can explain more severe masking criterion using *M2* (higher value of K_2). The distribution of the values of *M2* is asymmetric in both cases.

Fig. 9 illustrates that the average values of *M4* (relative vorticity) slightly increase with height for the flood episode and decrease for the second situation. This is probably caused by the fact that behind the cold front from the flood episode, there grew thermally caused surface pressure high.

6. CONCLUSION

The OFA applied to numerical data assessed the future development in the flood episode better than the methods of the classical synoptic meteorology because it could contribute to the timely reveal of the possibility of enhanced frontal precipitation amounts. This fact indicates that the OFA may be the one of useful means for the improvement of the general short-range weather forecast. On the other hand the situations of this type occur relatively often and are commonly accompanied with non-extreme precipitation amounts as in the second episode. Therefore, the satisfactory answer with regard to the significance of the OFA for the general short-range weather forecast will be obtained only after the application to the greater number of cases.

The technology of the OFA must be comprehended in a wider sense as the objective identification of atmospheric dynamical boundary-lines on various spatial scales. A significant example is the boundary of cold evaporative outflows from convective clouds. The OFA does not endeavour to simulate the classical synoptic procedures. It is possible only for the specific selection of the values of the masking threshold constants. The suitable assessment of the threshold constants enables an OFA application to the various types of problems, which can help at searching the causes of given state in the concrete case.

REFERENCES

[1] Berliner Wetterkarte 1995 and 1998 (in German). Institute für Meteorologie der Freien Universität Berlin.
[2] Bluestein, H. B. 1993. Synoptic-dynamic meteorology in midlatitudes. Vol. 2, Oxford University Press, INC.
[3] Daily Weather Views 1995 and 1998 (in Czech). Prague, Czech Hydrometeorological Institute (CHMI).
[4] Documentation of the EM/DM-System (1995). Version 1. Research Department, Deutscher Wetterdienst, Zentralamt, D-63004, Offenbach am Main.
[5] Hančarová, E., Metelka, L., Mrkvica, Z., Pavlík, J., Pozler, R., Šiftař, Z., Váchal, P., Veselý, R. (1999). Catastrophic flood in foothills of Orlické Hory mountains on July 22-25 1998 (in Czech). *Meteorol. Bulletin*, **1**, 1-12.
[6] Hewson, T. D. (1998a). Objective fronts. *Meteorol. Appl.* **5**. 37-65.
[7] Hewson, T. D. (1997). Objective identification of frontal wave cyclones. *Meteorol. Appl.* **4**. 311-315.
[8] Huber-Pock, F., Ch. Kress (1989). An operational model of objective frontal analysis based on ECMWF products, *Meteorol. Atmos. Phys.*, **40**, 170-180.
[9] Kakos, V., Řezáčová, D. (1999). Flash flood rains as viewed by meteorologists (in Czech). In '*Sborník referátů konference Orlice*'. 25-26 March 1999.
[10] Kašpar, M. (2000). Application of the objective front-plotting methodology to the area of Central Europe. Poster in European Geophysical Society XXV General Assembly 25-29 April, Nice, France.
[11] Renard, R. J., L. C. Clarke (1965). Experiments in numerical objective frontal analysis. *Mon. Wea. Rev.*, **93**, 547-556.
[12] Shapiro, R. (1970). Smoothing, Filtering, and Boundary Effects. *Rev. Geophysics and Space Physics.*, Vol. 8., **2**, 359-387.
[13] Sokol, Z. (1993). Objective analysis on a limited area. PhD Thesis, Math. and Phys. Faculty, Charles University, Prague. 135 pp. (in Czech).